Supplementary Table Legend

Table S1: Summary of sequencing Metadata. Related to Figure 1. Number of aligned reads, number of peaks, and sequencing protocol of each library, for Mbd3$^{f/-}$, Gatad2a$^{-/-}$, WT-1 and WT-2 engineered mouse reprogrammable systems.

Table S2: Gene expression values of 8042 differential genes in four different drug inducible reprogramming systems. Related to Figure 1. Calculated from PolyA+ RNA-seq, including protein-coding genes, pseudogenes, and lncRNAs, measured in the four different secondary reprogramming systems: Mbd3$^{f/-}$, Gatad2a$^{-/-}$, WT-1 and WT-2. Values are unit normalized FPKM (see **Methods**).

Table S3: Gene expression values of 8705 differential genes in Mbd3$^{f/-}$ system. Related to Figure 1. Gene expression values of 8705 differential genes in Mbd3$^{f/-}$ system, including polyA+ genes (protein-coding, pseudogenes, lncRNAs) and small RNA-seq (rRNA, miRNA, snoRNA). Values reported are FPKM.

Table S4: Differential lncRNA expression and OSKM binding during conducive naïve iPSC reprogramming trajectory. Related to Figure 1. Expanded lncRNA analysis beyond Ensemble annotation utilizing a PLAR-generated lncRNA dataset (see **Methods**). 560 differential lncRNA were identified during reprogramming, out of them 221 differential lncRNA not annotated in Ensembl. OSKM binding overlap, with associated Jaccard index, are included (same as presented in Fig. 1D).

Table S5: Clusters of enhancers with different demethylation dynamics. Related to Figure 3. Datasheet annotates clusters of enhancers with different demethylation dynamics as presented in **Fig. 3B**. Cluster 8 includes enhancers and super-enhancers with fast demethylation.

Table S6: ESPG and CAPG differential groups. Related to Figure 4. Detected differential gene groups during conducive iPSC reprogramming, including all differential genes and the differential genes subsets annotated as genes with epigenetically switched promoters (ESPGs) and genes with constitutively active promoters (CAPGs). Gene list is further divided to up-regulated and down-regulated list of each gene group.

Supplementary Material

Deterministic Somatic Cell Reprogramming Involves Continuous Transcriptional Changes Governed by Myc and Epigenetic-Driven Modules

Asaf Zviran[1,2*], Nofar Mor[1*], Yoach Rais[1*], Hila Gingold[1], Shani Peles[1], Elad Chomsky[1,3,4], Sergey Viukov[1], Jason D. Buenrostro[5,6], Roberta Scognamiglio[7], Leehee Weinberger[1], Yair S. Manor[1], Vladislav Krupalnik[1], Mirie Zerbib[1], Hadas Hezroni[3], Diego Adhemar Jaitin[8], David Larastiaso[8], Shlomit Gilad[9], Sima Benjamin[9], Ohad Gafni[1], Awni Mousa[1], Muneef Ayyash[1], Daoud Sheban[1], Jonathan Bayerl[1], Alejandro Aguilera Castrejon[1], Rada Massarwa[1], Itay Maza[1,10], Suhair Hanna[1,11], Yonatan Stelzer[13], Igor Ulitsky[3], William J. Greenleaf[13,14], Amos Tanay[3,4], Andreas Trumpp[7], Ido Amit[7], Yitzhak Pilpel[1], Noa Novershtern[1#] and Jacob H. Hanna[1#%].

*These authors contributed equally. #Senior authors.

#Correspondence: Jacob H. Hanna (jacob.hanna@weizmann.ac.il), Noa Novershtern (noa.novershtern@weizmann.ac.il), Yoach Rais (yoach.rais@weizmann.ac.il)

%Lead Contact

Figure S1

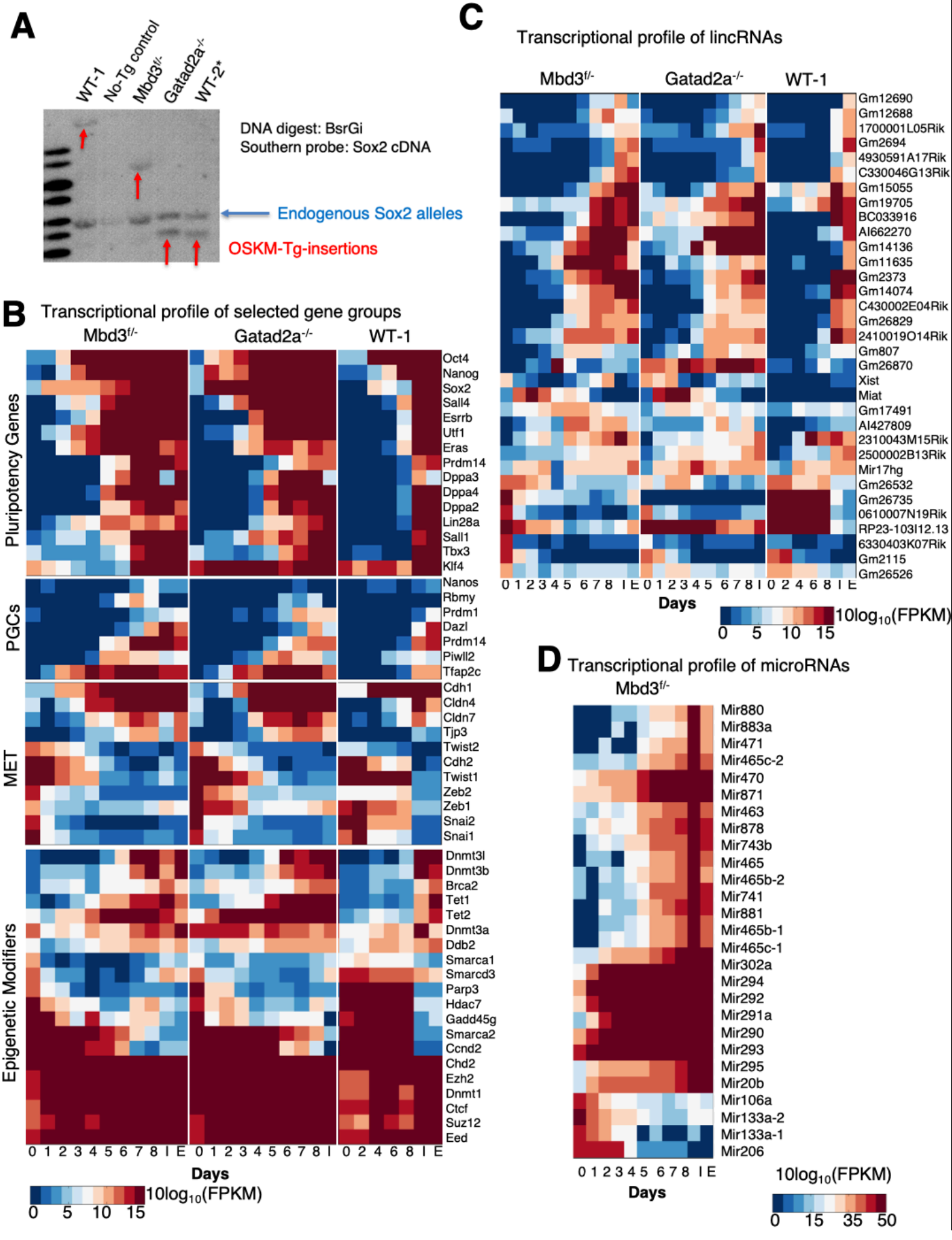
A
WT-1
No-Tg control
Mbd3f/-
Gatad2a-/-
WT-2*
DNA digest: BsrGi
Southern probe: Sox2 cDNA
Endogenous Sox2 alleles
OSKM-Tg-insertions
B
Transcriptional profile of selected gene groups
Mbd3f/-
Gatad2a-/-
WT-1
Pluripotency Genes
Oct4
Nanog
Sox2
Sall4
Esrrb
Utf1
Eras
Prdm14
Dppa3
Dppa4
Dppa2
Lin28a
Sall1
Tbx3
Klf4
PGCs
Nanos
Rbmy
Prdm1
Dazl
Prdm14
Piwll2
Tfap2c
MET
Cdh1
Cldn4
Cldn7
Tjp3
Twist2
Cdh2
Twist1
Zeb2
Zeb1
Snai2
Snai1
Epigenetic Modifiers
Dnmt3l
Dnmt3b
Brca2
Tet1
Tet2
Dnmt3a
Ddb2
Smarca1
Smarcd3
Parp3
Hdac7
Gadd45g
Smarca2
Ccnd2
Chd2
Ezh2
Dnmt1
Ctcf
Suz12
Eed
0 1 2 3 4 5 6 7 8 I E 0 1 2 3 4 5 6 7 8 I 0 2 4 6 8 I E
Days
10log10(FPKM)
0 5 10 15
C
Transcriptional profile of lincRNAs
Mbd3f/-
Gatad2a-/-
WT-1
Gm12690
Gm12688
1700001L05Rik
Gm2694
4930591A17Rik
C330046G13Rik
Gm15055
Gm19705
BC033916
AI662270
Gm14136
Gm11635
Gm2373
Gm14074
C430002E04Rik
Gm26829
2410019O14Rik
Gm807
Gm26870
Xist
Miat
Gm17491
AI427809
2310043M15Rik
2500002B13Rik
Mir17hg
Gm26532
Gm26735
0610007N19Rik
RP23-103I12.13
6330403K07Rik
Gm2115
Gm26526
0 1 2 3 4 5 6 7 8 I E 0 1 2 3 4 5 6 7 8 I 0 2 4 6 8 I E
Days
10log10(FPKM)
0 5 10 15
D
Transcriptional profile of microRNAs
Mbd3f/-
Mir880
Mir883a
Mir471
Mir465c-2
Mir470
Mir871
Mir463
Mir878
Mir743b
Mir465
Mir465b-2
Mir741
Mir881
Mir465b-1
Mir465c-1
Mir302a
Mir294
Mir292
Mir291a
Mir290
Mir293
Mir295
Mir20b
Mir106a
Mir133a-2
Mir133a-1
Mir206
0 1 2 3 4 5 6 7 8 I E
Days
10log10(FPKM)
0 15 35 50

Fig. S1: Continuous changes in specific gene groups of interest during the course of deterministic naïve iPSC reprogramming. Related to Fig. 1. **A.** Southern blot analysis for STEMCCA-OKSM integration in all lines used. Single copy integration was found in all lines used. Note that WT-2 and Gatad2a$^{-/-}$ have the same single copy integration pattern since these lines are isogenic and Gatad2a-KO by sgRNA was done at the final step after all transgenes and reporters were introduced. **B.** Transcription heatmap of Pluripotent genes, Primordial germ cell genes (PGCs), Mesenchymal to epithelial Transition (MET), and Epigenetic modifiers. Log_{10}(FPKM) values are presented in Mbd3$^{f/-}$, Gatad2a$^{-/-}$ and WT-1 systems. **C.** Transcription heatmap of differential lncRNAs, annotated according to mm10 (UCSC, December 2011). Log_{10}(FPKM) values are presented. **D.** Transcription heatmap of differential microRNAs (FC>600), measured using small-seq assay in Mbd3$^{f/-}$ system.

Figure S2

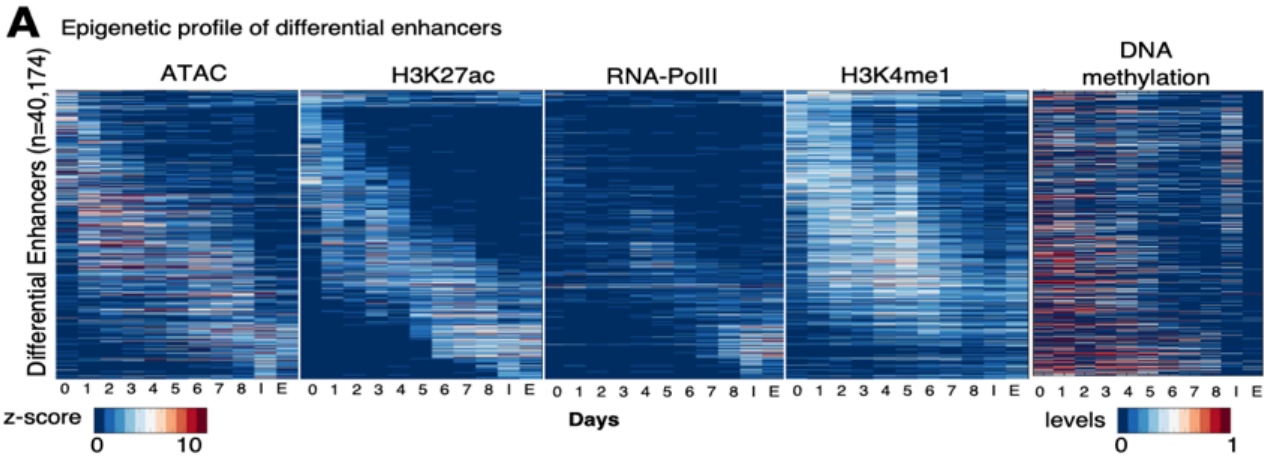
A
Epigenetic profile of differential enhancers
ATAC
H3K27ac
RNA-PolII
H3K4me1
DNA methylation
Differential Enhancers (n=40,174)
0 1 2 3 4 5 6 7 8 I E
z-score
0 10
Days
levels
0 1

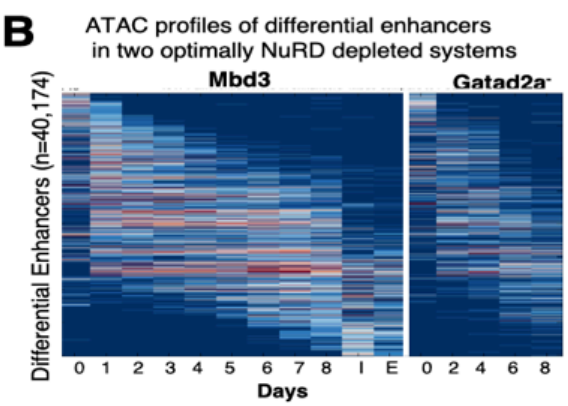
B
ATAC profiles of differential enhancers in two optimally NuRD depleted systems
Mbd3
Gatad2a-
Differential Enhancers (n=40,174)
0 1 2 3 4 5 6 7 8 I E
0 2 4 6 8
Days

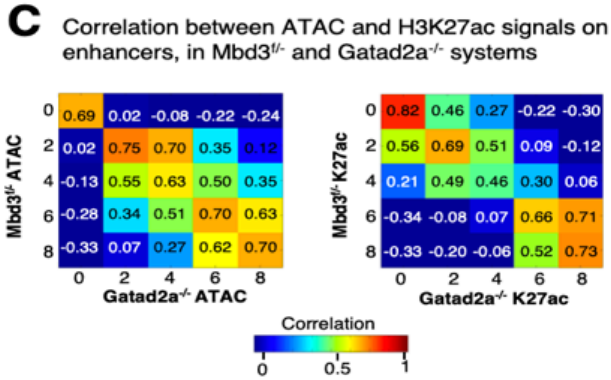
C
Correlation between ATAC and H3K27ac signals on enhancers, in Mbd3f/- and Gatad2a-/- systems
Mbd3f/- ATAC
0 2 4 6 8
0.69 0.02 -0.08 -0.22 -0.24
0.02 0.75 0.70 0.35 0.12
-0.13 0.55 0.63 0.50 0.35
-0.28 0.34 0.51 0.70 0.63
-0.33 0.07 0.27 0.62 0.70
Gatad2a-/- ATAC
Mbd3f/- K27ac
0.82 0.46 0.27 -0.22 -0.30
0.56 0.69 0.51 0.09 -0.12
0.21 0.49 0.46 0.30 0.06
-0.34 -0.08 0.07 0.66 0.71
-0.33 -0.20 -0.06 0.52 0.73
Gatad2a-/- K27ac
Correlation
0 0.5 1

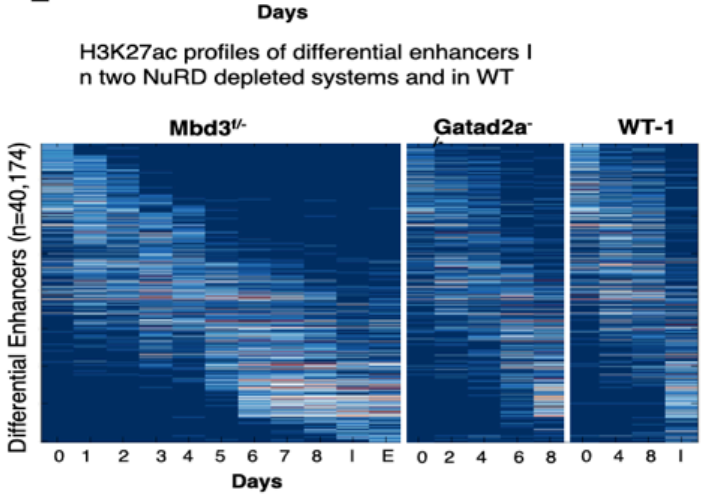
H3K27ac profiles of differential enhancers I n two NuRD depleted systems and in WT
Mbd3f/-
Gatad2a-
WT-1
Differential Enhancers (n=40,174)
0 1 2 3 4 5 6 7 8 I E
0 2 4 6 8
0 4 8 I
Days

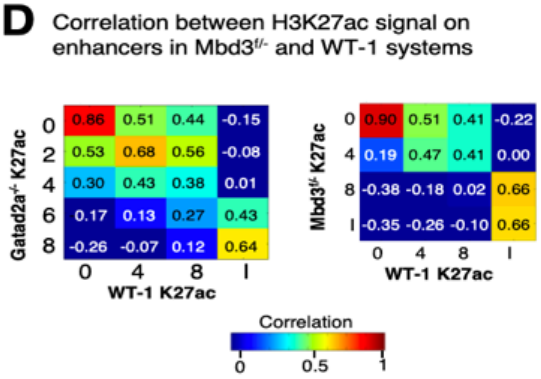
D
Correlation between H3K27ac signal on enhancers in Mbd3f/- and WT-1 systems
Gatad2a-/- K27ac
0 2 4 6 8
0.86 0.51 0.44 -0.15
0.53 0.68 0.56 -0.08
0.30 0.43 0.38 0.01
0.17 0.13 0.27 0.43
-0.26 -0.07 0.12 0.64
0 4 8 I
WT-1 K27ac
Mbd3f/- K27ac
0.90 0.51 0.41 -0.22
0.19 0.47 0.41 0.00
-0.38 -0.18 0.02 0.66
-0.35 -0.26 -0.10 0.66
Correlation
0 0.5 1

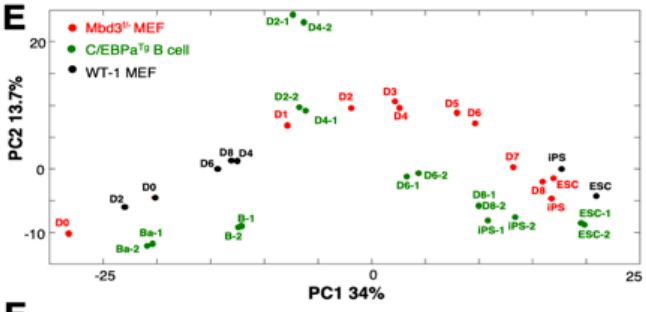
E
Mbd3f/- MEF
C/EBPaTg B cell
WT-1 MEF
PC2 13.7%
PC1 34%

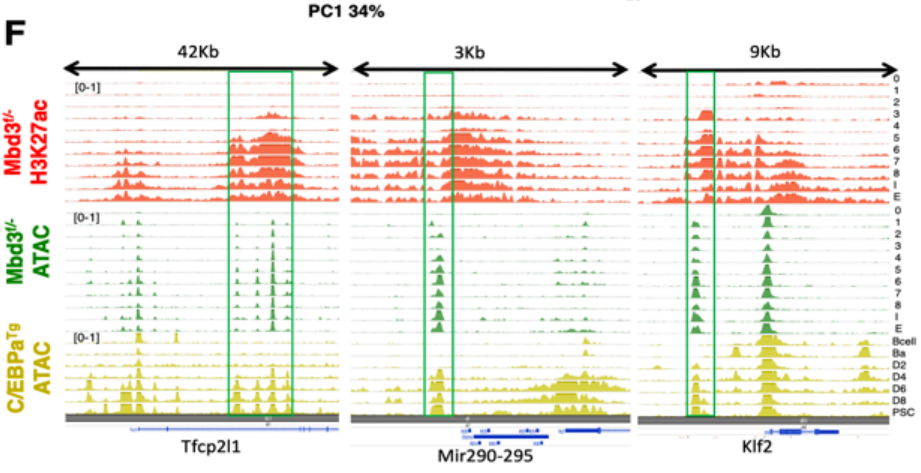
F
42Kb
3Kb
9Kb
Mbd3f/- H3K27ac
Mbd3f/- ATAC
C/EBPaTg ATAC
[0-1]
Tfcp2l1
Mir290-295
Klf2

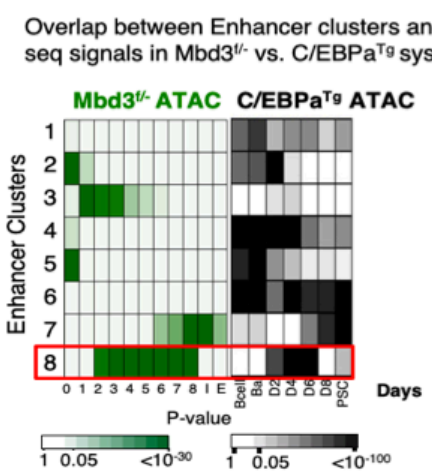
G
Overlap between Enhancer clusters and ATAC-seq signals in Mbd3f/- vs. C/EBPaTg systems
Mbd3f/- ATAC
C/EBPaTg ATAC
Enhancer Clusters
1 2 3 4 5 6 7 8
0 1 2 3 4 5 6 7 8 I E
Bcell Ba D2 D4 D6 D8 PSC
Days
P-value
1 0.05 <10-30
1 0.05 <10-100

Fig. S2: Massive epigenetic changes in enhancers detected during reprogramming. Related to Fig. 2. **A.** Profiles of 40,174 differential enhancers along reprogramming, showing H3K4me1, H3K27ac, DNA methylation, ATAC accessibility and PolII binding. **B.** DNA accessibility (Top) and H3K27ac (bottoms) signals of 40,174 differential enhancers (rows), in $Mbd3^{f/-}$, $Gatad2a^{-/-}$, and WT-1 systems. **C.** Spearman correlation matrix comparing DNA accessibility (left) and H3K27ac (right) measured on enhancers in $Mbd3^{f/-}$ and $Gatad2a^{-/-}$ systems. **D.** Spearman correlation matrix comparing H3K27ac measured on enhancers in $Mbd3^{f/-}$ and WT systems. H3K27ac enhancer profile in WT-1 day8 is more similar to $Mbd3^{f/-}$ day4, than to day8. **E.** PCA of transcriptional profiles of two efficient reprogramming systems: $Mbd3^{f/-}$ MEFs and $C/EBPa^{Tg}$ B cells (Stadhouders et al., 2018) calculated over 8042 differential expressed genes (Fig. 1d). PCA emphasizes that both efficient systems converge to ESC/iPSC profile, despite the fact that starting cells are different, and the trajectory is different. **F.** Landscape around three pluripotency related genes (Tfcp2l1, Mir290-295, Klf2), showing ATAC-seq signal as measured in two different systems - $Mbd3^{f/-}$ MEFs and $C/EBPa^{Tg}$ B cells (Stadhouders et al., 2018), as well as for H3K27ac signal. Enhancers, highlighted by green box, are activated in both systems, but in different kinetics: around day1-day2 in $Mbd3^{f/-}$ MEF system, and around day4 in $C/EBPa^{Tg}$ B cell system. Signals are normalized to sample size (RPM), and data range is indicated on top left corner of the signal. **G.** Enrichment of enhancer clusters, as shown in Figure 3**b**, for DNA accessibility in $Mbd3^{f/-}$ MEF and $C/EBPa^{Tg}$ B cell systems, showing that cluster 8 significantly overlaps regions that are accessible during intermediate days in both systems. This correlation matrix shows that both systems converge to PSC profile in eight days, with a slightly faster kinetics of $Mbd3^{f/-}$ system in the first 2 days. Color shades represent FDR corrected enrichment p-value.

Figure S3

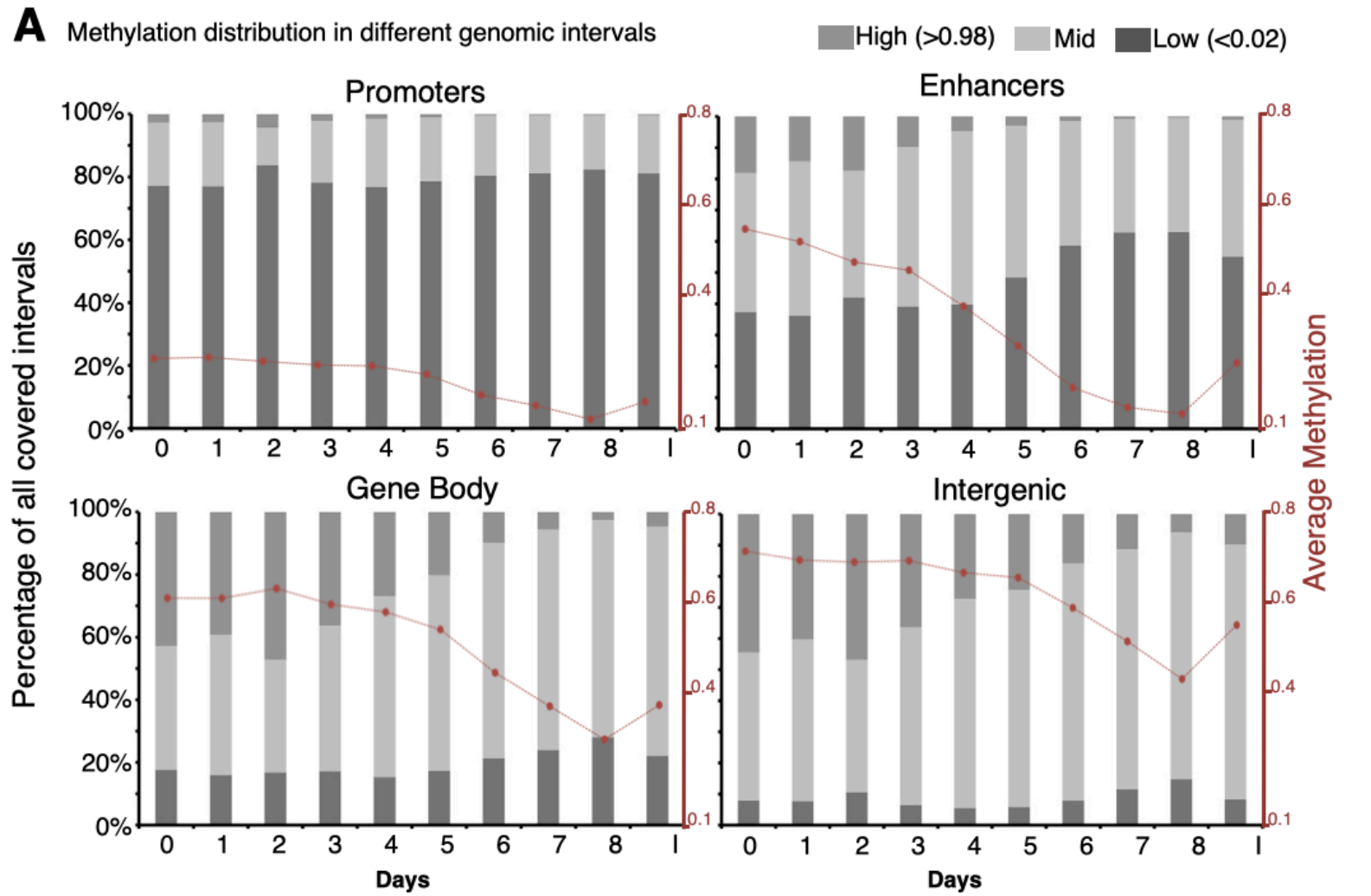
A
Methylation distribution in different genomic intervals
High (>0.98)
Mid
Low (<0.02)
Promoters
Enhancers
Gene Body
Intergenic
Percentage of all covered intervals
Average Methylation
Days
Days

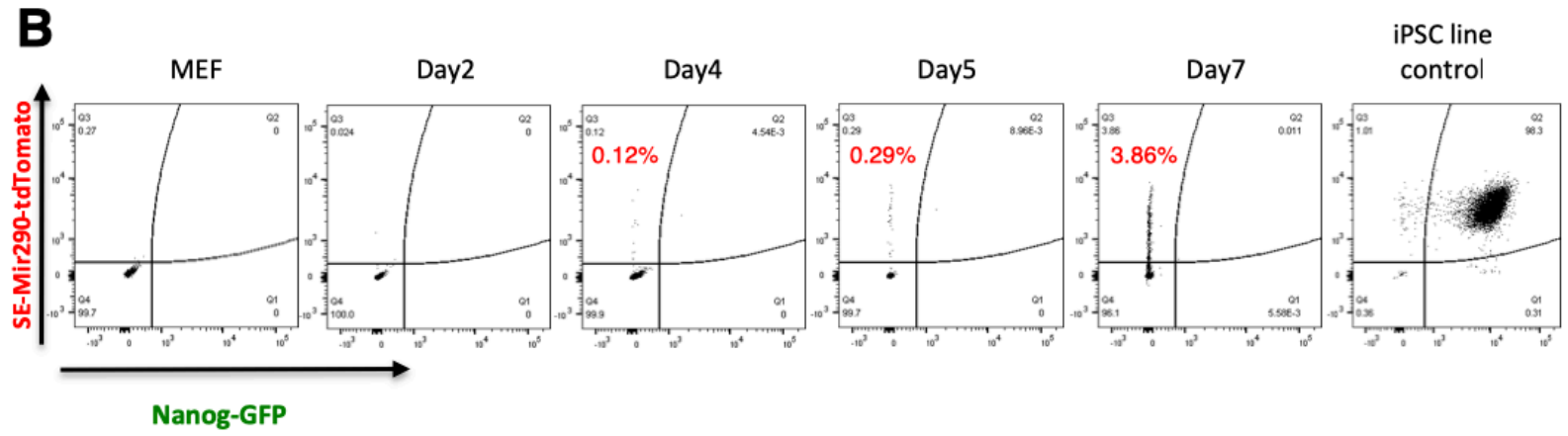
B
MEF
Day2
Day4
Day5
Day7
iPSC line control
0.12%
0.29%
3.86%
SE-Mir290-tdTomato
Nanog-GFP

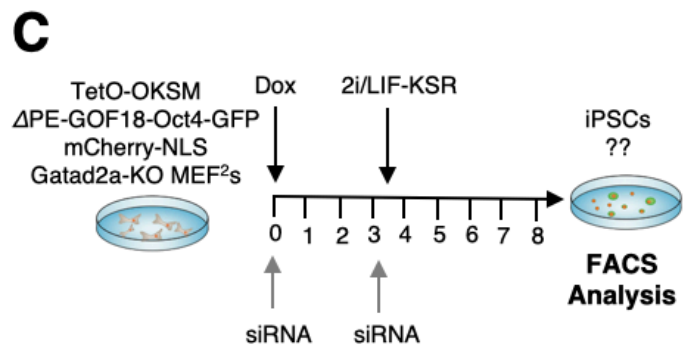
C
TetO-OKSM
ΔPE-GOF18-Oct4-GFP
mCherry-NLS
Gatad2a-KO MEF²s
Dox
2i/LIF-KSR
iPSCs
??
FACS Analysis
siRNA
siRNA

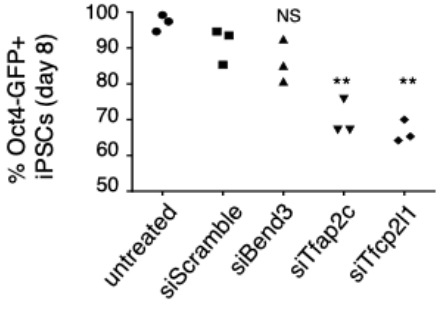
% Oct4-GFP+ iPSCs (day 8)
NS
untreated
siScramble
siBend3
siTfap2c
siTfcp2l1

Fig. S3: Global DNA demethylation changes during deterministic reprogramming. Related to Fig. 3. **A.** Distribution of low (<0.02), mid (0.02-0.98) and high (>0.98) methylation in four genomic regions: Promoters (1000bp around the TSS), Enhancers, Gene body (TSS to TES) and Intergenic regions (1000bp tiles), calculated in each day of reprogramming. **B.** Flow cytometry measurements of both Nanog-GFP reactivation and SE-Mir290-tdTomato during reprogramming of secondary fibroblasts. Sorting for RGM-Mir290-tdTomato+/Nanog-GFP- cells and double negative cells was done at day 5. Please note that single positive Nanog-GFP+ cells do not exist in naive reprogramming conditions as applied herein. **C.** Reprogramming efficiency (measured by Oct4 GFP+ cells percentage) was measured after 8 reprogramming days of Gatad2a-KO secondary MEF, following siRNA treatments targeting Tfcp2l and Tfap2c, on days 0 and 3. Both treatments resulted in 20-30% reduction of reprogramming efficiency comparing to control specimen (siScramble). ** $p<0.01$, Student t-test (n=3).

Figure S4

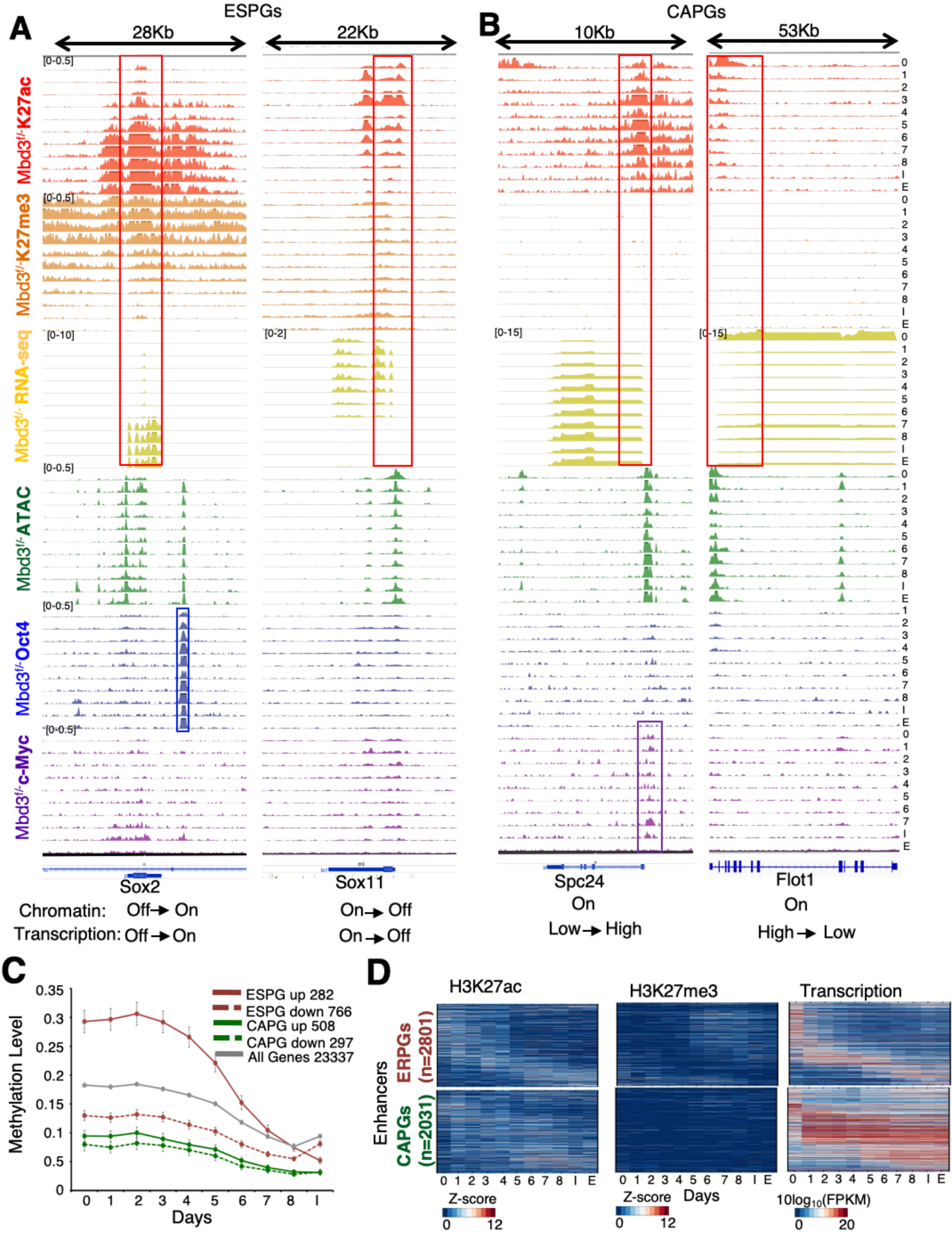
A
ESPGs
28Kb
22Kb
Mbd3f/-K27ac
Mbd3f/-K27me3
Mbd3f/- RNA-seq
Mbd3f/-ATAC
Mbd3f/-Oct4
Mbd3f/-c-Myc
[0-0.5]
[0-10]
[0-2]
Sox2
Sox11
Chromatin: Off→On
Transcription: Off→On
On→Off
On→Off
B
CAPGs
10Kb
53Kb
[0-15]
Spc24
On
Low→High
Flot1
On
High→Low
C
Methylation Level
Days
ESPG up 282
ESPG down 766
CAPG up 508
CAPG down 297
All Genes 23337
D
H3K27ac
H3K27me3
Transcription
Enhancers
ERPGs (n=2801)
CAPGs (n=2031)
Z-score
Days
10log10(FPKM)

Fig. S4: Different epigenetic landscape shown in ESPG and CAPG promoters and enhancers. Related to Fig. 4. **A.** ChIP-seq landscape showing binding of H3K27ac, H3K27me3, Oct4, c-Myc, alongside ATAC-seq and RNA-seq. Example of two genes with "epigenetically switched promoters" (ESPGs). Note that the change in H3K27ac and H3K27me3 corresponds to the change in expression (red box). Oct4 enhancer binding is highlighted in blue box **B.** Example of two genes with "consistently active promoters" (CAPGs). Note the constitutive high level of H3K27ac and low level of H3K27me3 regardless to the change in expression (red box). cMyc promoter binding is highlighted in purple box. Signals are normalized to sample size (RPM), and IGV data range is indicated on top left corner of the signal. **C.** DNA Methylation level of upregulated and downregulated ESPGs (red) and CAPGs (green), compared to all genes (gray), showing that CAPGs are hypomethylated, regardless of their expression pattern. **D.** Temporal profile of enhancer chromatin marks H3K27ac, H3K27me3, and gene expression of ESPGs and CAPGs that have an associated enhancer, along reprogramming. Each row corresponds to a single gene, genes are sorted according to their expression pattern and the same sorting was applied to the epigenetic marks in their corresponding enhancers.

Figure S5

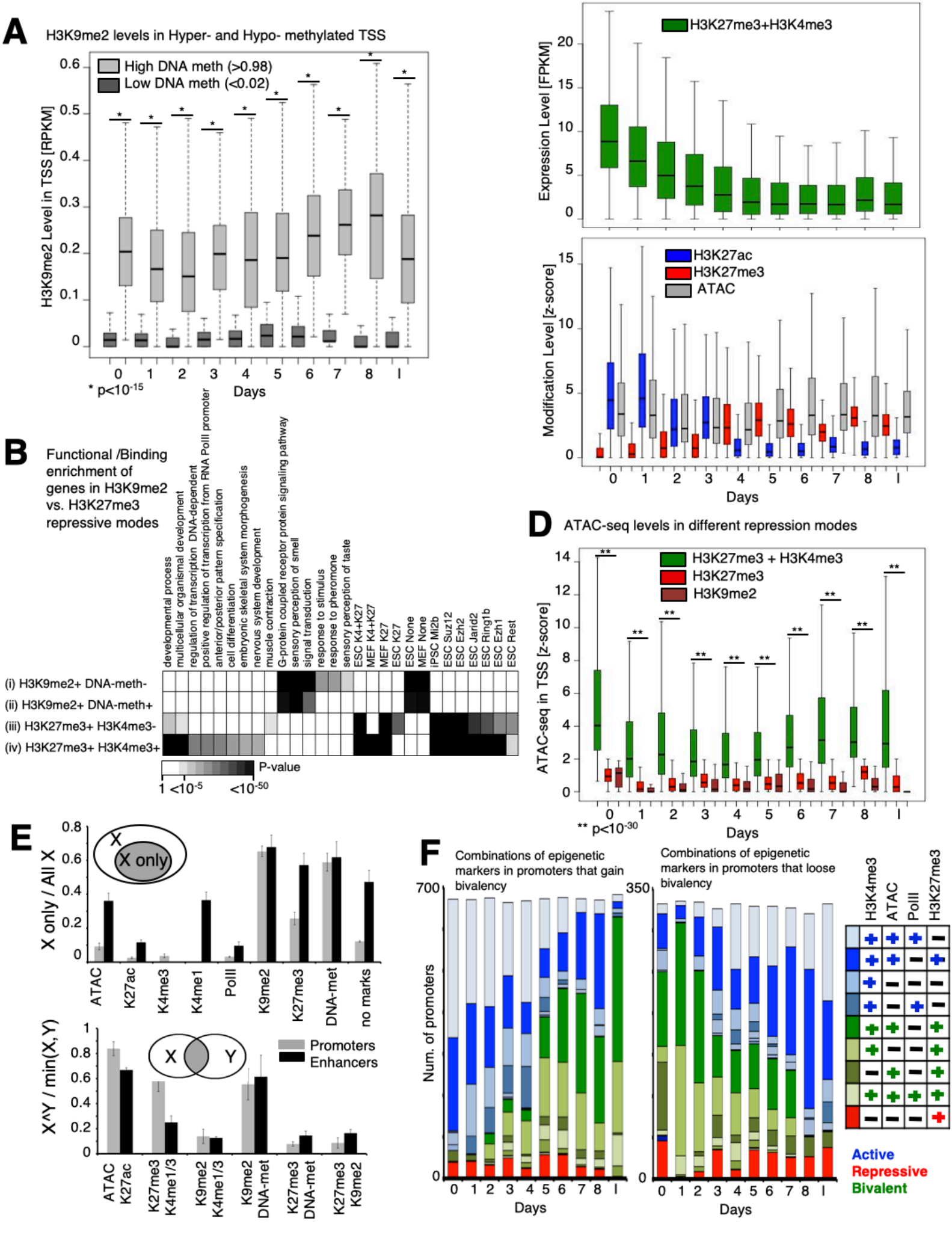
A
H3K9me2 levels in Hyper- and Hypo- methylated TSS
High DNA meth (>0.98)
Low DNA meth (<0.02)
H3K9me2 Level in TSS [RPKM]
* p<10-15
Days
B
Functional /Binding enrichment of genes in H3K9me2 vs. H3K27me3 repressive modes
developmental process
multicellular organismal development
regulation of transcription, DNA-dependent
positive regulation of transcription from RNA PolII promoter
anterior/posterior pattern specification
cell differentiation
embryonic skeletal system morphogenesis
nervous system development
muscle contraction
G-protein coupled receptor protein signaling pathway
sensory perception of smell
signal transduction
response to stimulus
response to pheromone
sensory perception of taste
ESC K4+K27
MEF K4+K27
MEF K27
ESC K27
ESC None
MEF None
iPSC Mi2b
ESC Suz12
ESC Ezh2
ESC Jarid2
ESC Ring1b
ESC Ezh1
ESC Rest
(i) H3K9me2+ DNA-meth-
(ii) H3K9me2+ DNA-meth+
(iii) H3K27me3+ H3K4me3-
(iv) H3K27me3+ H3K4me3+
P-value
1
<10-5
<10-50
C
Transcription and chromatin modification levels in bivalent genes
H3K27me3+H3K4me3
Expression Level [FPKM]
H3K27ac
H3K27me3
ATAC
Modification Level [z-score]
Days
D
ATAC-seq levels in different repression modes
H3K27me3 + H3K4me3
H3K27me3
H3K9me2
ATAC-seq in TSS [z-score]
** p<10-30
Days
E
X
X only
X only / All X
ATAC
K27ac
K4me3
K4me1
PolII
K9me2
K27me3
DNA-met
no marks
X
Y
Promoters
Enhancers
X^Y / min(X,Y)
ATAC K27ac
K27me3 K4me1/3
K9me2 K4me1/3
K9me2 DNA-met
K27me3 DNA-met
K27me3 K9me2
F
Combinations of epigenetic markers in promoters that gain bivalency
Combinations of epigenetic markers in promoters that loose bivalency
Num. of promoters
Days
H3K4me3
ATAC
PolII
H3K27me3
Active
Repressive
Bivalent

Fig. S5: H3K9me2 and H3K27me3 show functionally distinct modes of epigenetic repression during conducive reprogramming. Related to Fig. 5. **A.** Distribution of H3K9me2 signal in highly methylated (>0.98) and lowly methylated (<0.02) gene promoters, showing association of H3K9me2 with highly methylated promoters. * $p<10^{-15}$ (Wilcoxon test) **B.** Functional enrichment of genes marked by the indicated epigenetic marks in their promoters. Four gene groups were analyzed: (i) Genes with H3K9me2 without DNA-methylation (n=4159), (ii) Genes with both H3K9me2 and DNA methylation in at least two-time points (n=248), (ii) Genes with H3K27me3 without H3K4me3 (n=2220) and (iv) Genes with both H3K27me3 and H3K4me3 in at least two-time points (n=2663). Annotations include GO categories, targets of TF binding[46], or chromatin marks measured in ESC[75]. Gray shades indicate FDR corrected Fisher exact test p-values. Annotations with corrected p-value $<10^{-5}$ are presented. **C. Top:** Expression pattern of genes that gain bivalency during reprogramming (n=572). **Bottom:** Epigenetic modification level distribution of the same set of genes, showing a switch between H3K27ac and H3K27me3, and a constant state of accessibility. **D.** Chromatin accessibility of promoters marked by either repressive marks (H3K27me3, H3K9me2) or bivalent (H3K27me3+H3K4me3) modifications. Bivalent promoters are significantly more accessible than repressed promoters. ** $p<10^{-30}$ (Wilcoxon test). **E. Top:** Probability to observe the indicated epigenetic modification by its own in promoters (gray) and enhancers (black). **Bottom:** Probability to observe co-localized pairs of modifications in promoters and enhancers. **F.** Stacked bar chart of all combinations of the indicated chromatin modifications, as measured in promoters that gain bivalency (left) and in promoters that loose bivalency (right). Right – color code of frequent combinations (>3% of each sample).

Figure S6

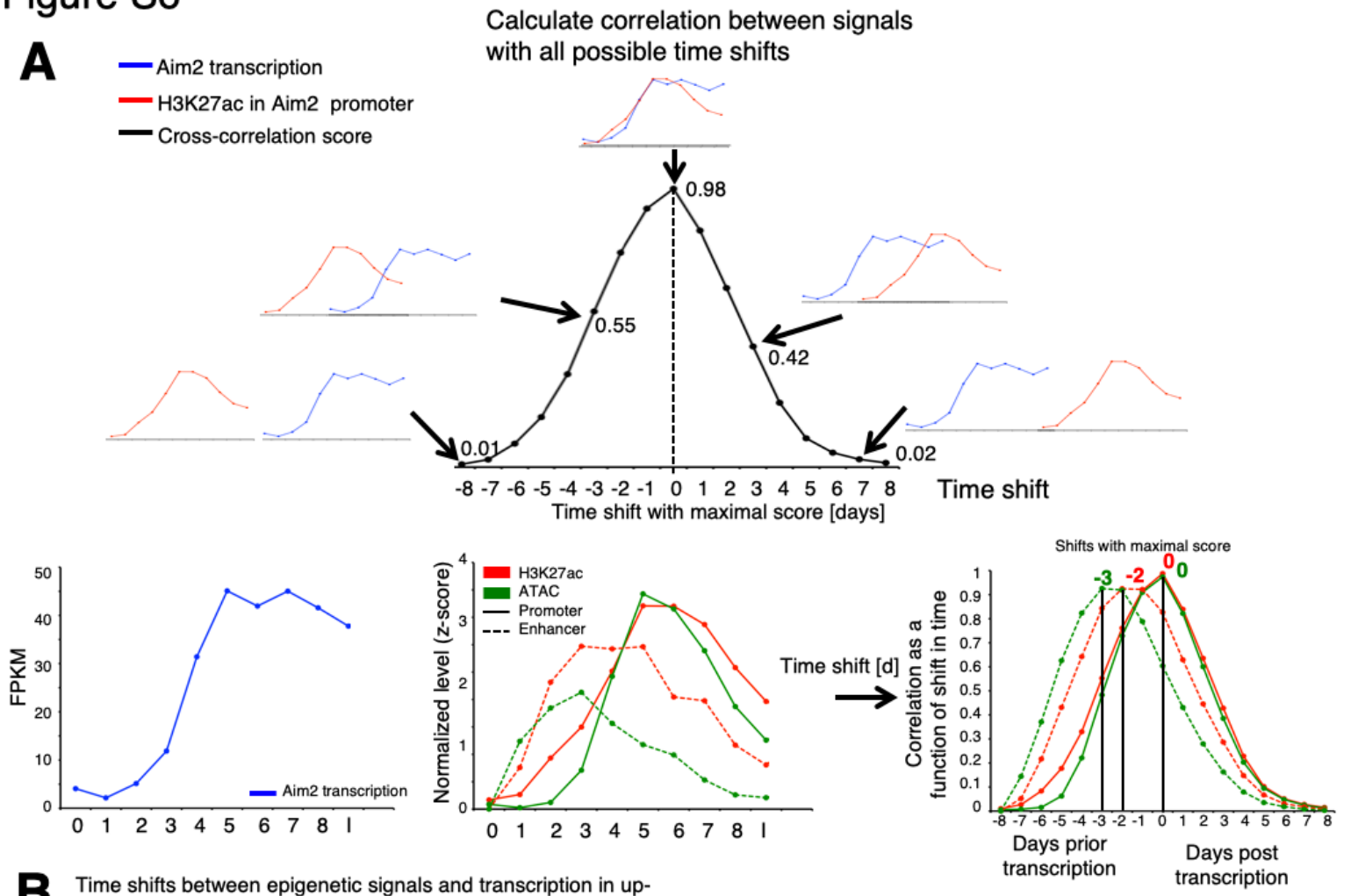
A
Aim2 transcription
H3K27ac in Aim2 promoter
Cross-correlation score
Calculate correlation between signals with all possible time shifts
0.98
0.55
0.42
0.01
0.02
Time shift
Time shift with maximal score [days]
FPKM
Aim2 transcription
Normalized level (z-score)
H3K27ac
ATAC
Promoter
Enhancer
Time shift [d]
Shifts with maximal score
Correlation as a function of shift in time
Days prior transcription
Days post transcription

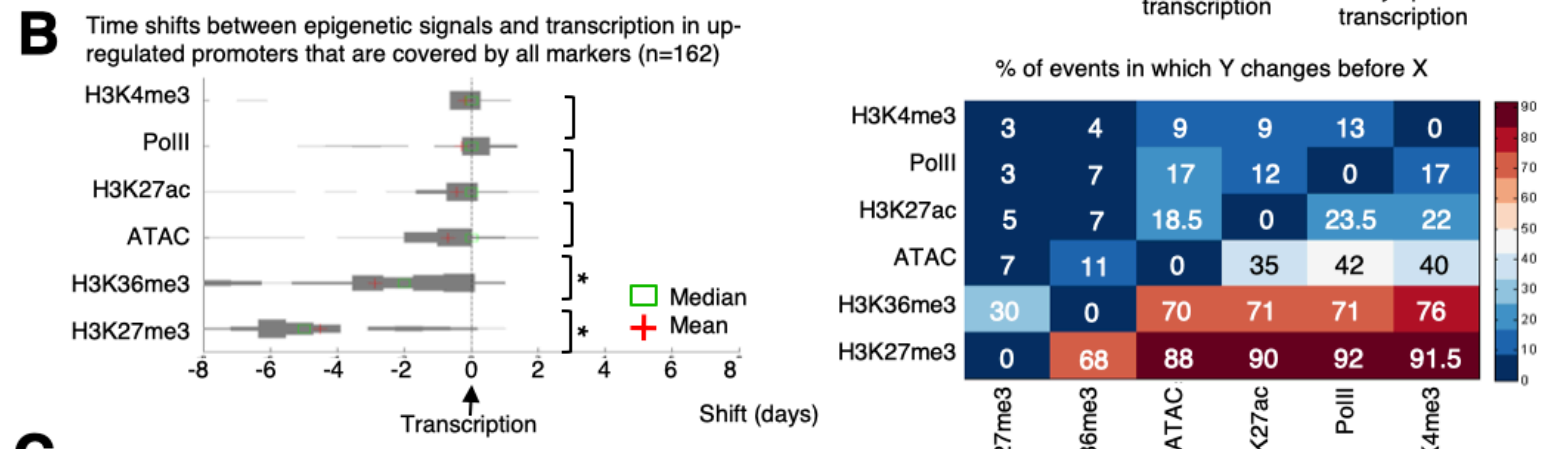
B
Time shifts between epigenetic signals and transcription in up-regulated promoters that are covered by all markers (n=162)
H3K4me3
PolII
H3K27ac
ATAC
H3K36me3
H3K27me3
Median
Mean
Transcription
Shift (days)
% of events in which Y changes before X
H3K4me3 3 4 9 9 13 0
PolII 3 7 17 12 0 17
H3K27ac 5 7 18.5 0 23.5 22
ATAC 7 11 0 35 42 40
H3K36me3 30 0 70 71 71 76
H3K27me3 0 68 88 90 92 91.5
H3K27me3 H3K36me3 ATAC H3K27ac PolII H3K4me3

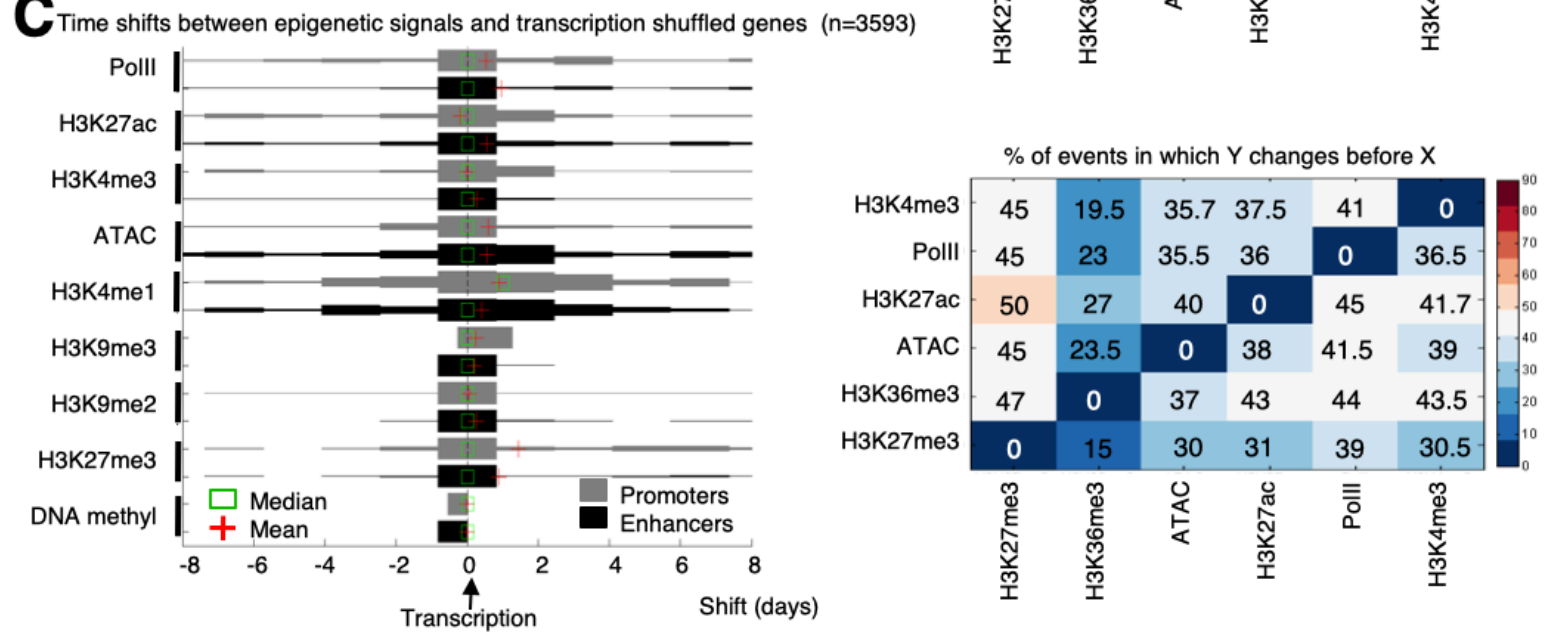
C
Time shifts between epigenetic signals and transcription shuffled genes (n=3593)
PolII
H3K27ac
H3K4me3
ATAC
H3K4me1
H3K9me3
H3K9me2
H3K27me3
DNA methyl
Median
Mean
Promoters
Enhancers
Transcription
Shift (days)
% of events in which Y changes before X
H3K4me3 45 19.5 35.7 37.5 41 0
PolII 45 23 35.5 36 0 36.5
H3K27ac 50 27 40 0 45 41.7
ATAC 45 23.5 0 38 41.5 39
H3K36me3 47 0 37 43 44 43.5
H3K27me3 0 15 30 31 39 30.5
H3K27me3 H3K36me3 ATAC H3K27ac PolII H3K4me3

Fig. S6: Utilizing cross-correlation method for inferring time shifts between chromatin epigenetic changes and mRNA transcription. Related to Fig. 5. **A. Top:** Cross correlation method[50,51] measures the overlap between two signals, while shifting the signals in their x-axis (convolution). In this case, the x-axis is time. The shift that gives the highest score is defined as the temporal offset between the signals. **Bottom:** example for cross-correlation method calculated in the promoter and enhancer of the gene Aim2. DNA accessibility and H3K27ac signal in promoter and enhancer are shown, alongside the shift of all signals from the transcription. **B. Left:** Distribution of cross-correlation temporal offset, measured between each of the indicated epigenetic modification and gene expression profile. The distribution was measured over 162 upregulated promoters that are covered by all indicated epigenetic modifications, thus comparing temporal offsets between epigenetic modifications on the same gene. Plus indicates mean, and square indicates median. * $p<10^{-5}$ (paired-sample ttest). **Right:** Matrix showing the percentage of events in which the modification on the Y axis changes before the modification on the X axis. Calculated over the same set of 162 promoters as on the left panel. This matrix emphasizes that the order of events in the promoters is removal of H3K27me3, followed by deposition of H3K36me3, opening of chromatin and then deposition of other active marks (H3K27ac, PolII, H3K4me3). **C. Left:** Shuffling analysis was done as a negative control for cross-correlation analysis: cross correlation temporal offset was calculated between each ESPGs gene expression (n=3593) and the indicated epigenetic modification taken randomly from another gene. Showing loss of temporal order with random promoter shuffling. **Right:** Matrix as in **(B)**, calculated over the shuffled promoters (n=3593), emphasizing the loss of order between the signals.

Figure S7

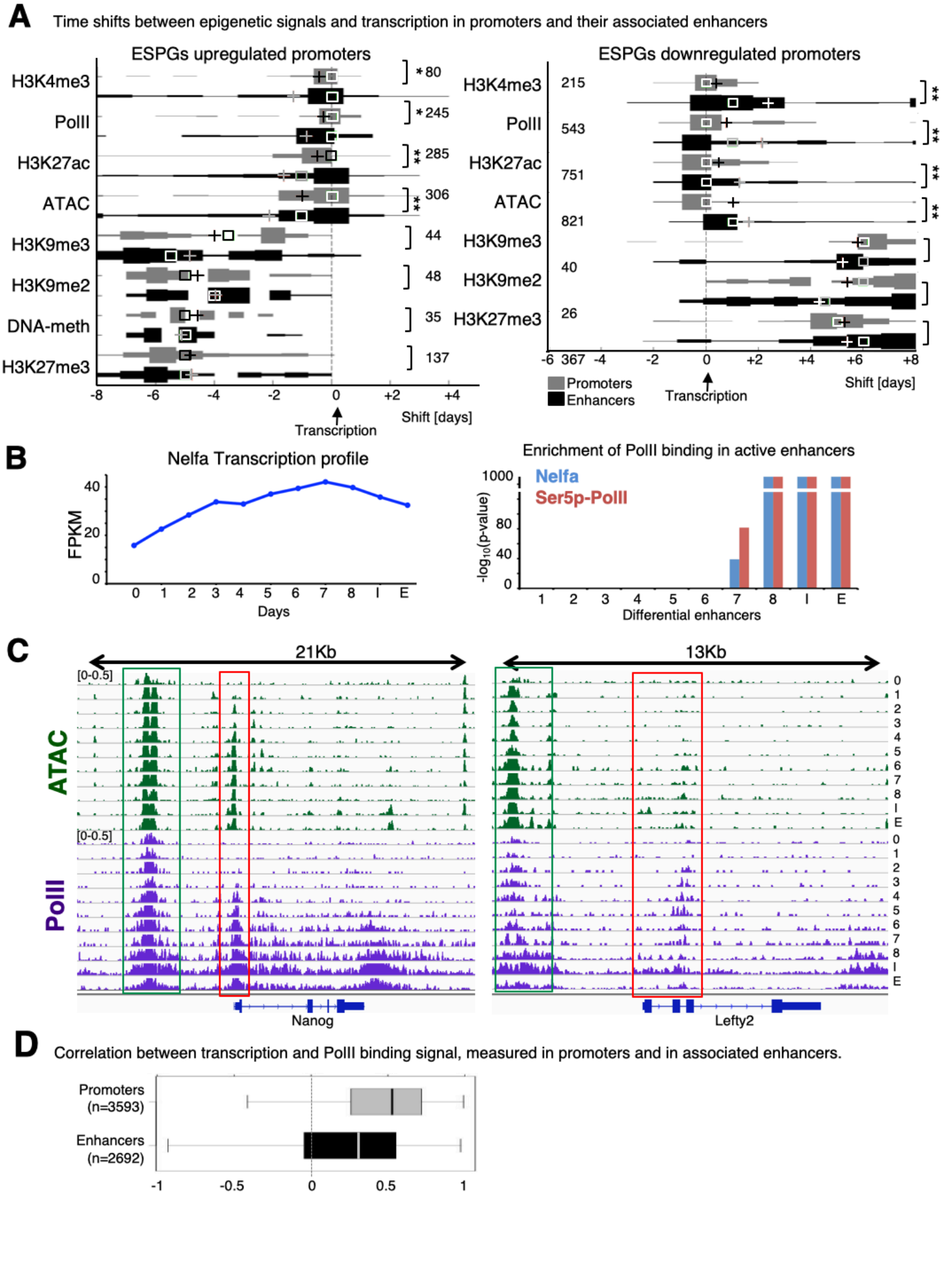
A
Time shifts between epigenetic signals and transcription in promoters and their associated enhancers
ESPGs upregulated promoters
H3K4me3
PolII
H3K27ac
ATAC
H3K9me3
H3K9me2
DNA-meth
H3K27me3
*80
*245
**285
**306
44
48
35
137
-8 -6 -4 -2 0 +2 +4
Transcription
Shift [days]
ESPGs downregulated promoters
H3K4me3
PolII
H3K27ac
ATAC
H3K9me3
H3K9me2
H3K27me3
215
543
751
821
40
26
**
**
**
**
-6 367 -4 -2 0 +2 +4 +6 +8
Promoters
Enhancers
Transcription
Shift [days]
B
Nelfa Transcription profile
FPKM
40
20
0
0 1 2 3 4 5 6 7 8 I E
Days
Enrichment of PolII binding in active enhancers
Nelfa
Ser5p-PolII
-log10(p-value)
1000
80
40
0
1 2 3 4 5 6 7 8 I E
Differential enhancers
C
21Kb
13Kb
ATAC
PolII
[0-0.5]
[0-0.5]
0 1 2 3 4 5 6 7 8 I E
0 1 2 3 4 5 6 7 8 I E
Nanog
Lefty2
D
Correlation between transcription and PolII binding signal, measured in promoters and in associated enhancers.
Promoters (n=3593)
Enhancers (n=2692)
-1 -0.5 0 0.5 1

Fig. S7: Enhancer activation and PolII enhancer binding precede activation and binding of associated promoter. Related to Fig. 5. **A.** Time shifts between the indicated chromatin modifications on promoter (gray) or associated enhancer (black) and gene expression, estimated with cross correlation method. The distribution was measured over all upregulated ESPGs (left) and downregulated ESPGs (right) which have a changing epigenetic modification (max-min z-score > 0.5) on both promoter and enhancer sites (numbers are indicated). Plus indicates mean, and square indicates median. * $p<10^{-2}$, ** $p<10^{-7}$ (Paired-sample t-test). **B. Left:** Expression pattern of PolII components Nelfa during conducive iPSC reprogramming. **Right:** enrichment of targets bound by Nelfa and Ser5p-PolII[27] among differential enhancers that are active in each day of reprogramming. $-\log_{10}$ of Fisher exact test p-values is indicated. **C.** Two cases in which PolII binds the enhancers before it binds the associated promoter. The enhancers are marked by a green box, promoters are marked by a red box. **D.** Correlation distribution between PolII binding signal and gene expression, as measured in promoters and in enhancers of ESPGs that are bound by PolII (numbers are indicated). Correlations were calculated for each gene, over 11 time points.